

# Lipid microdomains contribute to apoptosis-associated modifications of mitochondria in T cells

T Garofalo<sup>1,5</sup>, AM Giammarioli<sup>2</sup>, R Misasi<sup>1</sup>, A Tinari<sup>3</sup>,  
V Manganelli<sup>1</sup>, L Gambardella<sup>2</sup>, A Pavan<sup>4</sup>, W Malorni<sup>2,6</sup> and  
M Sorice<sup>\*,1,6</sup>

<sup>1</sup> Department of Experimental Medicine and Pathology, University of Rome 'La Sapienza', Rome, Italy

<sup>2</sup> Section of Cell Aging and Degeneration, Department of Drug Research and Evaluation, Rome, Italy

<sup>3</sup> Section of Ultrastructural Infectious Pathology, Department of Technology and Health, Istituto Superiore di Sanita', Rome, Italy

<sup>4</sup> Department of Experimental Medicine, University of L'Aquila, L'Aquila, Italy

<sup>5</sup> Laboratory of Experimental Medicine and Environmental Pathology, Rieti, Italy

<sup>6</sup> These authors contributed equally to this work as senior investigator

\* Corresponding author: M Sorice, Department of Experimental Medicine and Pathology, University of Rome 'La Sapienza', Viale Regina Elena 324, Rome 00161, Italy. Tel: +39-06-49972675; Fax: +39-06-4454820; E-mail: maurizio.sorice@uniroma1.it

Received 28.2.05; revised 12.4.05; accepted 18.4.05; published online 10.6.05  
Edited by JP Medema

## Abstract

Plasma membrane lipid microdomains have been considered as a sort of 'closed chamber', where several subcellular activities, including CD95/Fas-mediated proapoptotic signaling, take place. In this work we detected GD3 and GM3 gangliosides in isolated mitochondria from lymphoblastoid CEM cells. Moreover, we demonstrated the presence of microdomains in mitochondria by immunogold transmission electron microscopy. We also showed that GD3, the voltage-dependent anion channel-1 (VDAC-1) and the fission protein hFis1 are structural components of a multimolecular signaling complex, in which Bcl-2 family proteins (t-Bid and Bax) are recruited. The disruption of lipid microdomains in isolated mitochondria by methyl- $\beta$ -cyclodextrin prevented mitochondria depolarization induced by GD3 or t-Bid. Thus, mitochondrion appears as a subcompartmentalized organelle, in which microdomains may act as controllers of their apoptogenic programs, including fission-associated morphogenetic changes, megapore formation and function. These results disclose a new scenario in which mitochondria-associated lipid microdomains can act as regulators and catalysts of cell fate.

*Cell Death and Differentiation* (2005) 12, 1378–1389.

doi:10.1038/sj.cdd.4401672; published online 10 June 2005

**Keywords:** microdomains; gangliosides; mitochondria; apoptosis

**Abbreviations:** BSA, bovine serum albumin; COX-4, cytochrome *c* oxidase; Cyt *c*, cytochrome *c*;  $\Delta\Psi$ , mitochondrial membrane potential; DISC, death-inducing signaling complex; EGTA, ethylene glycol-bis-(aminoethyl ether) *N,N,N'*-tetraacetic acid; ER, endoplasmic reticulum; FCS, fetal calf serum; FITC,

fluorescein isothiocyanate; GEM, glycosphingolipid enriched microdomains; GM-130, Golgi marker 130; HPTLC, high-performance thin layer chromatography; HRP, horseradish peroxidase; LAMP-1, lysosome-associated membrane glycoprotein; M $\beta$ CD, methyl- $\beta$ -cyclodextrin; MoAb, monoclonal antibody; MOPS, 3[*N*-Morpholino] butane-sulfonic acid; PBS, phosphate-buffered saline; PKC, protein kinase C; PMSF, phenylmethylsulfonyl fluoride; PVDF, polyvinylidene difluoride; SB, swelling buffer; SDS-PAGE, sodium-dodecyl sulphate polyacrylamide gel electrophoresis; TEM, transmission electron microscopy; TMRM, tetramethylrhodamine-methyl-ester-perchlorate; VDAC-1, voltage-dependent anion channel-1

## Introduction

Gangliosides, sialic acid-containing glycosphingolipids, are ubiquitous constituents of cell plasma membrane. Recent lines of evidence also indicated that they are associated to intracellular organelles, including the Golgi apparatus and a subcompartment of the endoplasmic reticulum termed 'mitochondria-associated membrane'.<sup>1</sup> In addition, the presence of a metabolic pathway of sphingolipids, including several enzyme activities of sphingolipid metabolism, has been described in mitochondria.<sup>2</sup> The cell expression pattern of gangliosides depends on the cell type. In human lymphocytic cells monosialoganglioside GM3 is the main constituent<sup>3</sup> and disialoganglioside GD3 is also well expressed. These molecules are mainly concentrated in glycosphingolipid-enriched microdomains (GEM), where they are complexed with several proteins implied in signal transduction,<sup>4</sup> such as tyrosine kinase receptors, glycosyl-phosphatidylinositol-anchored proteins, Src-like tyrosine kinases (Lck, Lyn, Fyn), protein kinase C isozymes and, after T cell activation, the Syk family kinase Zap-70.<sup>5</sup> During apoptosis, the death-inducing signaling complex (DISC) associates with these domains upon CD95/Fas engagement.<sup>6,7</sup> In particular, a role for gangliosides as structural components of the multimolecular signaling complex involved in CD95/Fas receptor-mediated apoptotic pathway was suggested.<sup>6</sup> Although not all cell types show the raft-dependency of CD95/Fas clustering,<sup>7,8</sup> in lymphocytic cells, the GEM-dependency of the initiation of receptor clustering and signaling was demonstrated by using cholesterol depleting agents, such as methyl- $\beta$ -cyclodextrin (M $\beta$ CD).<sup>9</sup> In addition, it was hypothesized<sup>10,11</sup> that a portion of intracellular GD3 can play a role in apoptotic machinery. Activation of death receptors (CD95/Fas, TNF $\alpha$  receptor) induces an intracellular flow of GD3, probably carried entirely by raft-containing vesicular transport.<sup>12</sup> GD3 synthesis increased and the ganglioside concentration decreased from the cell surface via raft-dependent endocytosis and moved via vesicular transport towards the mitochondria.<sup>13</sup> Thus, GD3 has been reported to propagate CD95/Fas-mediated apoptotic signals<sup>10,14</sup> and act on the mitochondrial permeability transition pore, leading to cytochrome *c* (Cyt *c*) release.<sup>15,16</sup>

However, the actual role of the GD3 action and its subcellular targets still remain to be elucidated.

The role of mitochondrial fission and fusion processes has recently been taken into consideration in the apoptotic cell death process.<sup>17</sup> It has been hypothesized that the fusion process could be associated with cell senescence and survival, while the mitochondrial fission process may occur in cells undergoing apoptosis. Fusion and fission processes are instructed by a series of molecules.<sup>17</sup> Among these, h-Fis seems to play a key role.<sup>17,18</sup> This was described as an integral protein of the outer mitochondrial membrane participating to the membrane scission events. Members of the sphingomyelin pathway seem to have a profound influence on the apoptotic cascade, including these mitochondrial changes.<sup>19</sup> The present study was thus undertaken to ascertain whether the dynamic mitochondriotropic redistribution of GD3 could bolster mitochondrial subcompartmentalization hijacking human T cells towards a CD95/Fas apoptotic prone phenotype.

## Results

### Evidence for the existence of GD3-enriched microdomains in mitochondria

In the first set of experiments, the existence of GD3 enriched microdomains in the mitochondria of human lymphoblastoid CEM cells was assessed.

Scanning confocal microscopic analysis of GD3 expression and distribution revealed that anti-GD3 staining appeared uneven and punctate over the plasma membrane of either untreated (Figure 1A, panel a), or anti-CD95/Fas-treated cells (Figure 1A, panel b), but, importantly, it also revealed an intracellular GD3 localization (Figure 1A, panels c and d, respectively) clearly referred to specific cytoplasmic compartments, that is, to mitochondria. In fact, the merged image obtained by anti-GD3 monoclonal antibodies (MoAbs) together with a mitochondria-specific dye (Figure 1A, panels e and f) clearly revealed yellow-orange areas, resulting from the overlap of green and red fluorescence, which corresponded to nearly complete colocalization areas. These overlaid areas were much more evident in CD95/Fas crosslinked CEM cells (Figure 1A, panel h) with respect to control samples where co-localization (yellow-orange) areas was negligible (Figure 1A, panel g). These experiments were performed with two different fixation and permeabilization methods, 0.5% Triton X-100 and acetone-methanol (1 : 1, v/v), which gave virtually similar results, according to our previous papers.<sup>11,20</sup> The presence of GD3 molecules in mitochondria was confirmed by high-performance thin layer chromatography (HPTLC) analysis of total gangliosides, which revealed in isolated mitochondria the presence of two main resorcinol-positive bands, comigrating with GM3 and GD3, respectively (Figure 1B). It indicates that mitochondria from CEM cells show a less complex ganglioside pattern as compared to whole cells.<sup>6</sup> Densitometric analysis revealed a significant increase of GD3 content in mitochondria after triggering through CD95/Fas (Figure 1C). Conversely, a decrease of GD3 content was observed in the supernatant withdrawn of mitochondria. The identity of the GD3 comigrating band was

confirmed by TLC immunostaining, using a highly specific anti-GD3 MoAb (not shown). The purity of the mitochondrial preparations was assessed by Western blot by checking lysosome-associated membrane glycoprotein (LAMP-1), Golgi marker 130 (GM-130), Transferrin receptor and subunit IV of COX-IV (Figure 1D).

Immunogold labeling of thin sections clearly indicated the presence of GD3 molecules in control untreated cells, forming well evident clusters at the plasma membrane while no gold labeling was detectable at mitochondrial level (Figure 2a). By contrast, the analysis of CD95/Fas treated cells clearly indicated that GD3-positive gold particle clusters were observable not only on the cell surface (Figure 2b, inset) but also as packed aggregates in the cell cytoplasm (Figure 2b). More interestingly, in treated cells, gold particles were detectable in mitochondria (Figure 2c), forming well organized structures associated with the internal cristae (Figure 2d, inset). Quantitative evaluation of mitochondrial GD3 staining was also carried out. In Figure 2e, the results obtained from EM morphometric analyses are shown. A significant difference was detected between control and treated cells, since gold particles localized mainly at the plasma membrane in control samples and at mitochondrial level in treated cell samples.

### Lipid microdomains localization of voltage-dependent anion channel (VDAC-1)/porin

Since it was hypothesized that GD3 induces opening of the permeability transition pore in isolated mitochondria,<sup>21</sup> we analyzed the possible interaction between GD3 and VDAC-1. VDAC proteins constitute the major pathway for metabolic exchange across the mitochondrial outer membrane and are candidate components of the permeability transition pore, thought to participate in apoptotic cell death.<sup>22</sup>

Thus, cell-free lysates from anti-CD95/Fas-treated and untreated cells were immunoprecipitated with anti-VDAC-1 MoAb, followed by protein A-acrylic beads. Acidic glycosphingolipids were extracted from the VDAC-1 immunoprecipitates and analyzed by HPTLC. The analysis revealed two resorcinol-positive bands, comigrating with GM3 and GD3 in both untreated and treated cells (Figure 3a). The identity of the latter band as GD3 was confirmed by TLC immunostaining, using the anti-GD3 MoAb, which revealed in untreated cells a GD3 band, which became more evident after triggering through CD95/Fas. It demonstrated an interaction between GD3 and VDAC-1. The immunoprecipitation was verified by Western blot. As a control for the specificity of the protein-ganglioside interaction, cell-free lysates from anti-CD95/Fas-treated and untreated cells were also immunoprecipitated with anti-Bid and analyzed as above. Acidic glycosphingolipids were extracted from the Bid immunoprecipitates and analyzed by HPTLC. No resorcinol-positive bands were revealed in both untreated and treated cells (Figure 3b). The immunoprecipitation was verified by Western blot. This finding is consistent with the observation that Bid is specifically associated with different lipid molecules.<sup>23</sup>

To analyze the presence of VDAC-1 in the GEM fraction of CEM cells, we investigated the distribution of this protein in

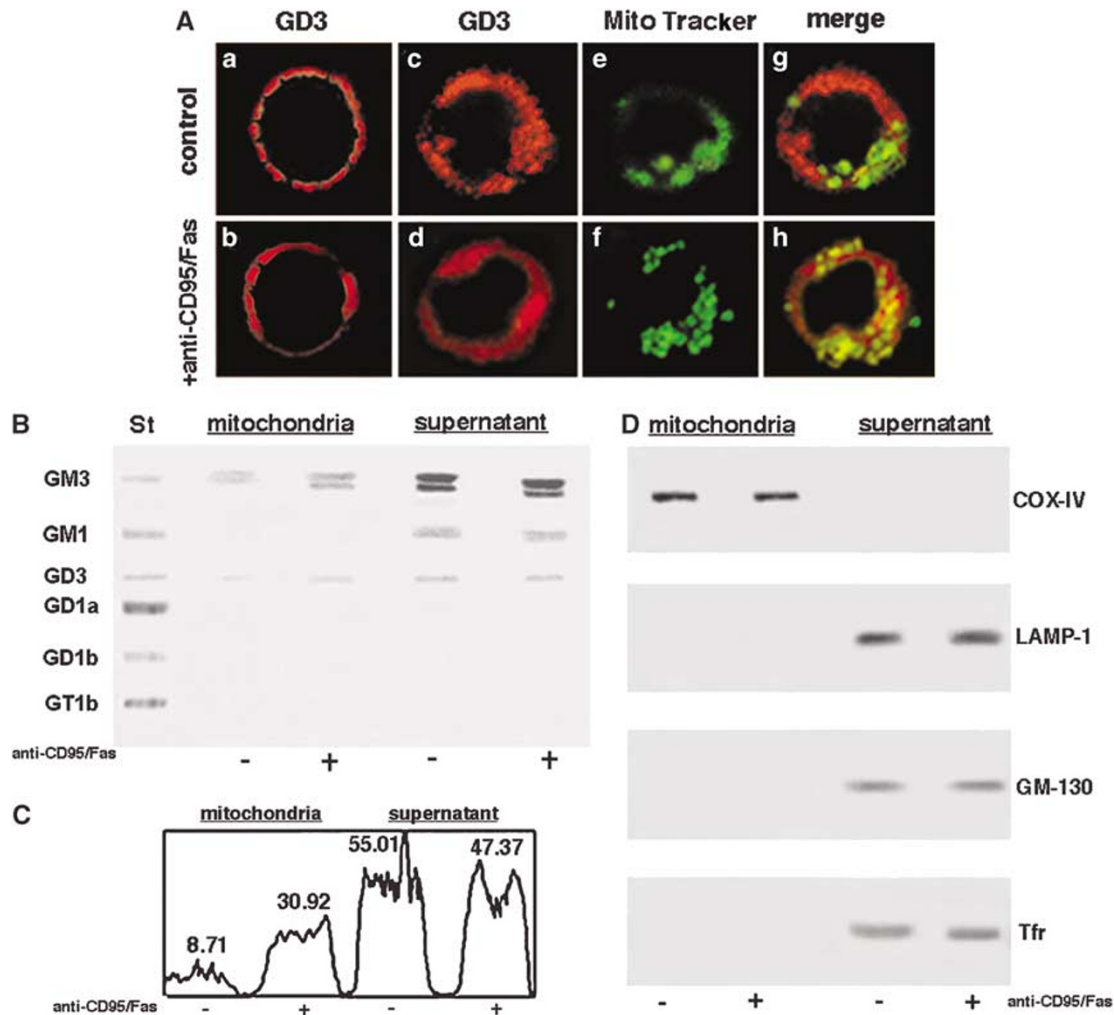


**Figure 1** Evidence for the existence of GD3-enriched microdomains in mitochondria. **(A)** CEM cells were fixed with 4% formaldehyde in PBS for 30 min at 4°C and labeled with GMR19 anti-GD3 MoAb for 1 h at 4°C, followed by three washes in PBS and addition (1 h at 4°C) of Texas Red-conjugated anti-mouse IgM. Apoptosis was induced by incubating cells with anti-CD95/Fas (250 ng/ml for 1 h at 37°C). (a) Plasma membrane GD3 staining of untreated cells; (b) plasma membrane GD3 staining of anti-CD95/Fas treated cells. CEM cells were also stained with Mito Tracker Green FM for 2 h at 37°C; cells were fixed with 4% paraformaldehyde, permeabilized with 0.5% Triton X-100 and incubated with anti-GD3 MoAb and then with Texas red-conjugated anti-mouse IgM. (c) GD3 staining of untreated cells; (d) GD3 staining of anti-CD95/Fas treated cells; (e) Mito Tracker staining of untreated cells; (f) Mito Tracker staining of anti-CD95/Fas treated cells; (g) dual immunolabeling of GD3 and Mito Tracker of untreated cells; (h) dual immunolabeling of GD3 and Mito Tracker of anti-CD95/Fas treated cells. The images were acquired with a scanning confocal microscope, collected at 512 × 512 pixels and processed with the Leica confocal software 4.7. To note that yellow-orange areas, indicating overlay of mitochondria and GD3 labeling are well detectable in CD95-treated cells only (h). Colocalization areas are stained in yellow. **(B)** HPTLC analysis of the ganglioside pattern of mitochondria from CEM cells, untreated or treated with anti-CD95/Fas. Gangliosides were extracted from isolated mitochondria and from the supernatant withdrawn of mitochondria in chloroform/methanol/water. St: standard gangliosides GM3, GM1, GD3, GD1a, GD1b, GT1b. The plate was stained with resorcinol (ganglioside-specific stain). **(C)** densitometric scanning analysis of the GD3 comigrating bands detected by Mac OS 9.0, using NIH Image 1.62 software. **(D)** Western blotting of mitochondria and supernatant performed with MoAbs against LAMP-1, GM-130, Transferrin receptor or COX-IV. The same amounts of proteins for each sample were run

fractions obtained by a 5–30% linear sucrose gradient in the absence or in the presence of crosslinking with anti-CD95/Fas antibody (Figure 3c). The results revealed that in both untreated and anti-CD95/Fas-treated cells, VDAC-1 was present mainly in fractions 5–6. To demonstrate that VDAC-1 was present in mitochondrial lipid microdomains, we performed the same analysis in both Triton X-100-insoluble and -soluble fractions obtained from isolated mitochondria. Again, we found the presence of VDAC-1 in the detergent-insoluble fraction of both untreated and anti-CD95/Fas treated cells, although it was also present in the Triton X-100 soluble

fraction (Figure 3d). Hence, VDAC-1 was constitutively present in lipid microdomains of CEM cells mitochondria.

### Lipid microdomains localization of Bax and t-Bid proteins after triggering through CD95/Fas

We subsequently investigated whether these microdomains were directly involved in cell apoptosis. With this aim, we focused primarily on the Bcl-2 family death promoters Bax and Bid, which represent indispensable effectors of the apoptotic

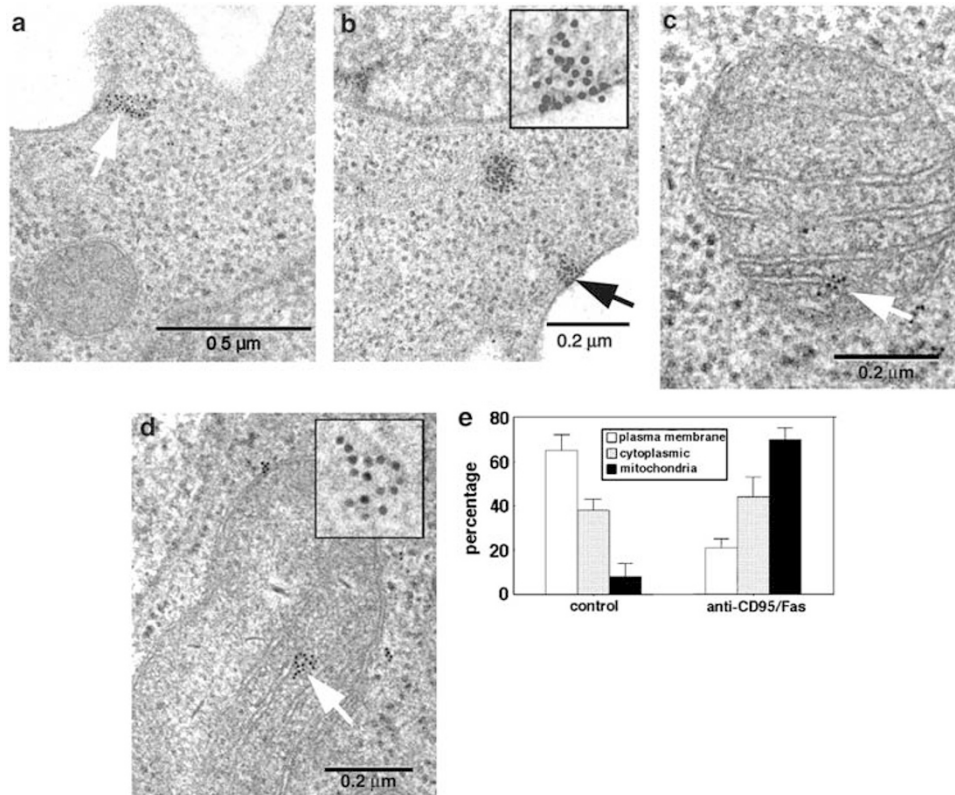


**Figure 2** Immunogold labeling of GD3. A membrane-associated labeling is detectable in control samples (a). To note that no gold particles are observable in the mitochondria. In CD95/Fas treated cells, the gold particles are visible at the plasma membrane (b, arrow) as well as a cytoplasmic aggregate (b). Note the absence of a membrane delimiting the particle cluster. Inset in (b) shows, at higher magnification, the distribution of GD3 molecules that appears specifically localized on the membrane leaflet as well as just beneath the plasma membrane. In CD95/Fas treated cells, gold particles are also observable associated with mitochondrial membranes (c, arrow) also forming small aggregates (d, arrow). Inset shows the well-arranged distribution of gold particles at higher magnification. One example representative of three different experiments. TEM morphometric analyses (e) show significant differences ( $P < 0.01$ ) in gold particle localization. They are mainly visible at the plasma membrane in control samples and at mitochondrial level in treated cell samples. By contrast, no significant difference was detected at cytoplasmic level

pathway.<sup>24</sup> In particular, Bax, in association with Bid, may promote VDAC opening or form a VDAC-Bax hybrid channel that releases Cyt *c*.<sup>25,26</sup> Thus, we also analyzed the distribution of these proteins in fractions obtained by a 5–30% linear sucrose gradient, after different incubation times with anti-CD95/Fas. As shown in Figure 4a, in unstimulated cells, Bax was present in fractions 8–11, but was virtually absent in fractions 4–6, corresponding to lipid microdomains. However, the protein became progressively less soluble in the detergent after triggering through CD95/Fas. In fact, Bax was detected in the detergent insoluble fractions 4–6. In isolated mitochondria from the same cells, Bax recruited to Triton X-100 fraction after triggering through CD95/Fas (Figure 4c).

Furthermore, we analyzed the distribution of Bid, a proapoptotic protein of the Bcl-2 family that acts directly on mitochondrial membranes to facilitate the release of apoptogenic factors.<sup>27</sup> Bid was almost entirely present in Triton-X-100 soluble fractions of untreated cells (Figure 4b). Indeed, the full-length protein was present mainly in fractions 8–11. Conversely, after anti-CD95/Fas cross-linking, Bid was processed into the active form (truncated Bid, t-Bid), and, interestingly, it was present in the fraction 5 only (GEM fraction). This finding was confirmed in isolated mitochondria.

These experiments revealed that the active t-Bid recruited to Triton X-100-insoluble fraction (Figure 4d), supporting the view that t-Bid recruited to mitochondrial lipid microdomains, upon CD95/Fas crosslinking.

### Association of fission protein hFis1 with mitochondrial lipid microdomains

We analyzed the possible association of hFis1 with mitochondrial lipid microdomains. The analysis of the distribution of the fission protein hFis1 in fractions obtained by a 5–30% linear sucrose gradient revealed that hFis1 was enriched in fractions 4–6, corresponding to lipid microdomains (Figure 5a). This enrichment became more evident after triggering through anti-CD95/Fas, as revealed by densitometric analysis (Figure 5b). In the same vein, intensified video microscopy (IVD) (Figure 5c–f), as well as scanning confocal microscopy analyses (not shown), clearly indicated: (i) the localization of hFis1 to cell mitochondria in untreated cells (Figure 5c), as well as to fragmented mitochondria in anti-CD95/Fas-treated cells (Figure 5d); (ii) the GD3-hFis1 association, revealed by yellow areas, which corresponded to colocalization areas (Figure 5e, f). These areas were significantly more evident in anti-CD95/Fas treated cells (Figure 5f) with respect to

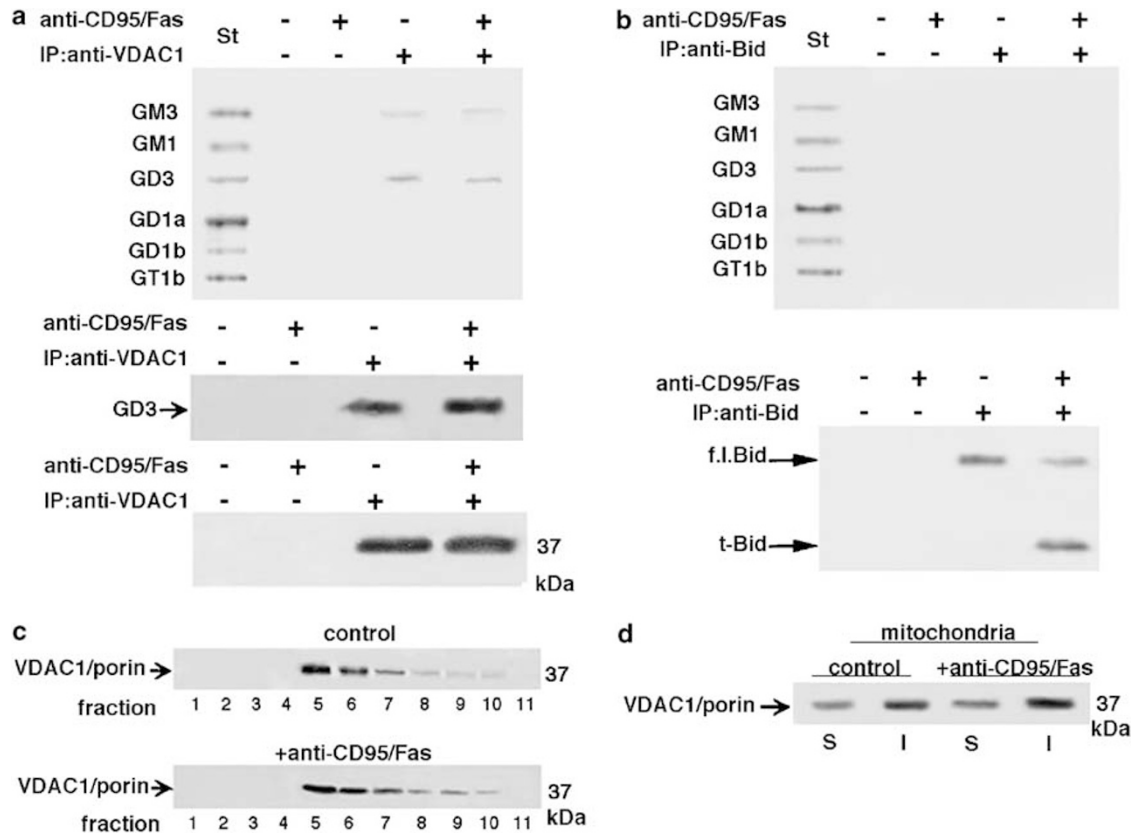


**Figure 3** Lipid microdomains localization of VDAC-1/porin. (a) CEM cells, untreated or treated with anti-CD95/Fas (250 ng/ml for 1 h at 37°C), were lysed in lysis buffer, followed by immunoprecipitation with goat anti-VDAC-1/porin. A goat IgG isotypic control was employed. The immunoprecipitates were run on HPLC plates and stained with resorcinol. Alternatively, the immunoprecipitates were analyzed for the presence of GD3 by TLC immunostaining analysis, using an anti-GD3 MoAb (GMR19). A control of immunoprecipitates was assessed by immunoblot with anti-VDAC-1/porin. (b) CEM cells, untreated or treated with anti-CD95/Fas (250 ng/ml for 1 h at 37°C), were lysed in lysis buffer, followed by immunoprecipitation with anti-Bid. A rabbit IgG isotypic control was employed. The immunoprecipitates were run on HPLC plates and stained with resorcinol. As a control, immunoprecipitates were assessed by immunoblot with anti-Bid. (c) VDAC-1/porin distribution in lymphoblastoid CEM cells. CEM cells, either untreated or treated with anti-CD95/Fas, were lysed and the supernatant fraction was subject to sucrose density gradient. After centrifugation, the gradient was fractionated and each gradient fraction was recovered and analyzed by Western blotting with an anti-VDAC-1/porin polyclonal Ab. (d) Isolated mitochondria from CEM cells, either untreated or treated with anti-CD95/Fas, were detergent solubilized as reported in the 'Materials and Methods'. Both Triton X-100-soluble and -insoluble fractions were analyzed by Western blot and probed with anti-VDAC-1/porin polyclonal Ab

untreated cells (Figure 5e). These findings suggest that CD95/Fas triggering induces the lateral reorganization of mitochondrial lipid microdomains, bringing hFis1 together with GD3.

### Effect of MβCD on mitochondria depolarization induced by GD3 or t-Bid

To analyze the contribution of mitochondrial lipid microdomains in GD3-regulated apoptosis, we evaluated changes occurring in membrane potential of isolated mitochondria after GD3 incubation. Consistent with previous works,<sup>10,21</sup> flow cytometric analysis showed that ganglioside GD3 was able to induce *per se* a significant loss of mitochondrial membrane potential ( $\Delta\Psi$ ) (Figure 6a).

Furthermore, experiments were also carried out by pre-incubating isolated mitochondria with MβCD, since this compound is known to induce cholesterol efflux from the membrane and, consequently, microdomain disruption.

Although mitochondria contain low levels of cholesterol as compared to other organelles,<sup>24,25,28,29</sup> this compound was able to affect the free cholesterol in isolated mitochondria, as revealed by TLC analysis (Figure 6e). Indeed, after MβCD treatment of isolated mitochondria, the total free cholesterol content was about 55% that found in MβCD untreated mitochondria (Figure 6f). Interestingly, MβCD significantly prevented (about 50%) the GD3-triggered loss of  $\Delta\Psi$  (Figure 6b), suggesting that lipid microdomains play a key role in GD3-mediated effect leading to cell apoptosis. In parallel experiments we analyzed the contribution of mitochondrial lipid microdomains in the activity of Bid. In particular, since we have above demonstrated that t-Bid targets mitochondrial lipid microdomains, we first analyzed the effect of t-Bid on  $\Delta\Psi$  of isolated mitochondria and, subsequently, we evaluated the effects of MβCD on this important apoptosis-associated parameter. Our results showed that pretreatment with MβCD (Figure 6d) reduced up to 50%, the percentage of depolarized mitochondria induced by t-Bid (Figure 6c). These results clearly suggest that t-Bid-induced  $\Delta\Psi$  loss during

apoptosis could depend on its interaction with mitochondrial lipid microdomains. Finally, we have also evaluated Cyt *c* release by isolated mitochondria (Figure 6g) after treatment with GD3 given alone (c) or following M $\beta$ CD administration (d). As controls, parallel mitochondrial preparations were treated with M $\beta$ CD (b) or t-Bid given alone (e), or after M $\beta$ CD administration (f). The results obtained clearly indicated a significantly higher release of the Cyt *c* apoptogenic molecule by GD3- and t-Bid-treated mitochondria with respect to M $\beta$ CD treated samples (b, d, f).

## Discussion

Microdomains at the plasma membrane have been considered preferential sites on the cell plasma membrane,<sup>30</sup> where several subcellular activities take place.<sup>6</sup> In particular, they may be involved in the control of apoptosis via positive interactions involving CD95/Fas or via negative interactions involving Bad.<sup>31,32</sup> Indeed, some apoptotic molecules, such as CD95/Fas, FADD, procaspase-8 and procaspase-10 are recruited into microdomains,<sup>33</sup> whereas relocalization of Bad from lipid rafts to mitochondria resulted in apoptosis.<sup>32</sup> In the present work we bolster the role played by microdomains in the cell death program by introducing a novel task for gangliosides. In fact, the arrangement of GD3 molecules at the plasma membrane, well visible in control cells, was strongly modified by CD95/Fas triggering. Clusters and aggregates were in fact detectable in the cell cytoplasm and in the mitochondria. Thus, according to biochemical literature data hypothesizing a redistribution of GD3 molecule after apoptotic triggering,<sup>13</sup> we showed for the first time by immunogold transmission electron microscopy (TEM) analyses that GD3 molecules can effectively be detectable as associated with mitochondria. These ultrastructural results allowed us to hypothesize that intracytoplasmic trafficking of GD3 molecules from the plasma membrane, through the cell cytoplasm, to the mitochondria can also take place. A role in this trafficking of GD3 molecules towards mitochondria may be played by actin cytoskeleton microfilaments, namely by ezrin molecule, which was shown to associate with GD3 after CD95/Fas triggering.<sup>11</sup> Furthermore, structural, well-organized features of GD3-positive clusters in different cell compartments including mitochondria (see the inset in Figure 2d) seem also to be suggestive for the ability of GD3 molecule to instruct a sort of mitochondrial 'closed chamber' where specific reactions can take place. In particular, our results strongly suggest that these highly dynamic structures could be specialized portions of mitochondrial membranes contributing to the instruction of the apoptotic execution cascade, where may eventually translocate proteins, which relocate from plasma membrane lipid rafts to mitochondria following apoptotic triggering.<sup>31</sup>

Till now, it was hypothesized that GD3 can contribute to the apoptotic program by directly targeting mitochondria in a Bcl-2-controlled manner and inducing the mitochondrial release of apoptogenic factors.<sup>15</sup> Our results provide the first evidence that GD3 acts at the level of the VDAC, where a local perturbation of specific mitochondrial lipid microdomains influencing the permeability transition pore complex and Cyt

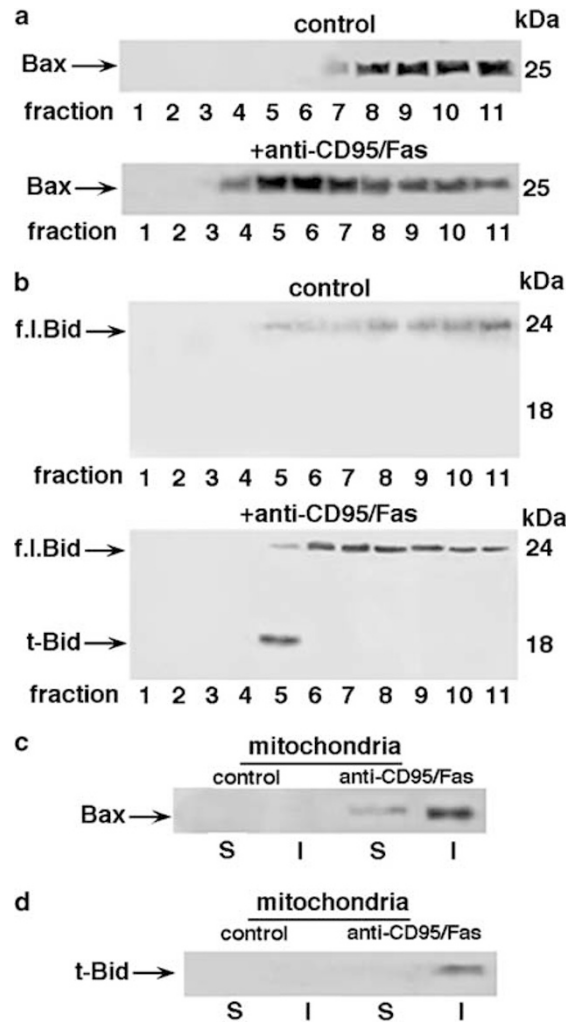


**Figure 4** Lipid microdomains localization of Bax and t-Bid proteins. CEM cells, either untreated or treated with anti-CD95/Fas (250 ng/ml for 1 h at 37 °C), were lysed and the supernatant fraction was subject to sucrose density gradient. After centrifugation, the gradient was fractionated and each gradient fraction was recovered and analyzed by Western blotting. (a) Fractions obtained after sucrose density gradient, either untreated or treated with anti-CD95/Fas, were analyzed using an anti-Bax MoAb. (b) Fractions obtained after sucrose density gradient, either untreated or treated with anti-CD95/Fas, were analyzed using an anti-Bid polyclonal Ab. (c) Isolated mitochondria from CEM cells, either untreated or treated with anti-CD95/Fas, were detergent solubilized as reported in the 'Materials and Methods'. Both Triton X-100-soluble and -insoluble fractions were analyzed by Western blot and probed with anti-Bax MoAb. (d) Isolated mitochondria from CEM cells, either untreated or treated with anti-CD95/Fas, were detergent solubilized as reported in the 'Materials and Methods'. Both Triton X-100-soluble and -insoluble fractions were analyzed by Western blot and probed with the anti-Bid polyclonal Ab

*c* release occurs. In this concern, a relevant role may be played by Bax and t-Bid, which relocate to lipid microdomains, as revealed by the analysis of linear sucrose gradient fractions from whole cells. Furthermore, since previous analyses reported that several mitochondrial proteins may be Triton X-100-insoluble, using suitable detergent/protein ratio,<sup>34</sup> we analyzed the proteins under test in both Triton X-100-insoluble and -soluble fractions from isolated mitochondria. Our results further underlined the recruitment of selective proteins to

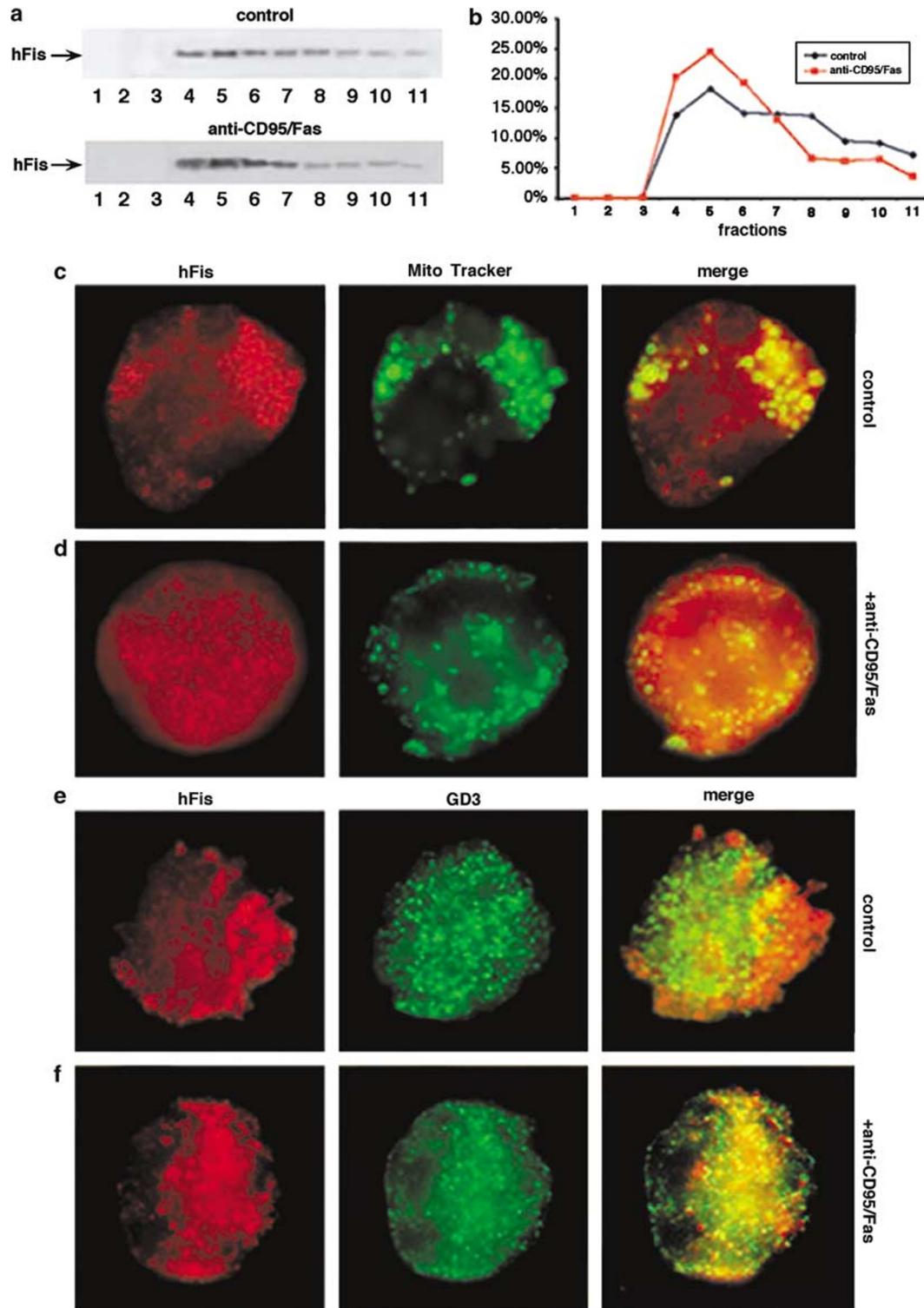


**Figure 5** Association of fission protein hFis1 with mitochondrial lipid microdomains. **(a)** hFis1 distribution in CEM sucrose gradient fractions. CEM cells, untreated or treated with anti-CD95/Fas, 250 ng/ml for 1 h at 37°C, were lysed in lysis buffer and the supernatant fraction was subjected to sucrose density gradient. After centrifugation, the gradient was fractionated and each gradient fraction was recovered and analyzed by Western blotting with anti-hFis1 polyclonal Ab. **(b)** Percent distribution across the gel of the 11 fractions in untreated (black line) and anti-CD95/Fas-treated cells (red line), as detected by densitometric scanning analysis. **(c, d)** IVM analysis of hFis1-mitochondria association in CEM cells. Cells were stained with Mito Tracker Green FM for 2 h at 37°C; apoptosis was induced by incubating cells with anti-CD95/Fas. Cells were fixed with 4% paraformaldehyde, permeabilized with 0.5% Triton X-100 and incubated with anti-hFis1 polyclonal Ab and then with Texas red-conjugated anti-rabbit IgG. Colocalization areas are stained in yellow. **(e, f)** IVM analysis of hFis1-GD3 association in CEM cells. Cells, untreated or treated with anti-CD95/Fas, were fixed with 4% paraformaldehyde, permeabilized with 0.5% Triton X-100 and incubated with anti-hFis1 plus Texas red-conjugated anti-rabbit IgG and then with anti-GD3 MoAb plus FITC-conjugated anti-mouse IgM. Colocalization areas are stained in yellow

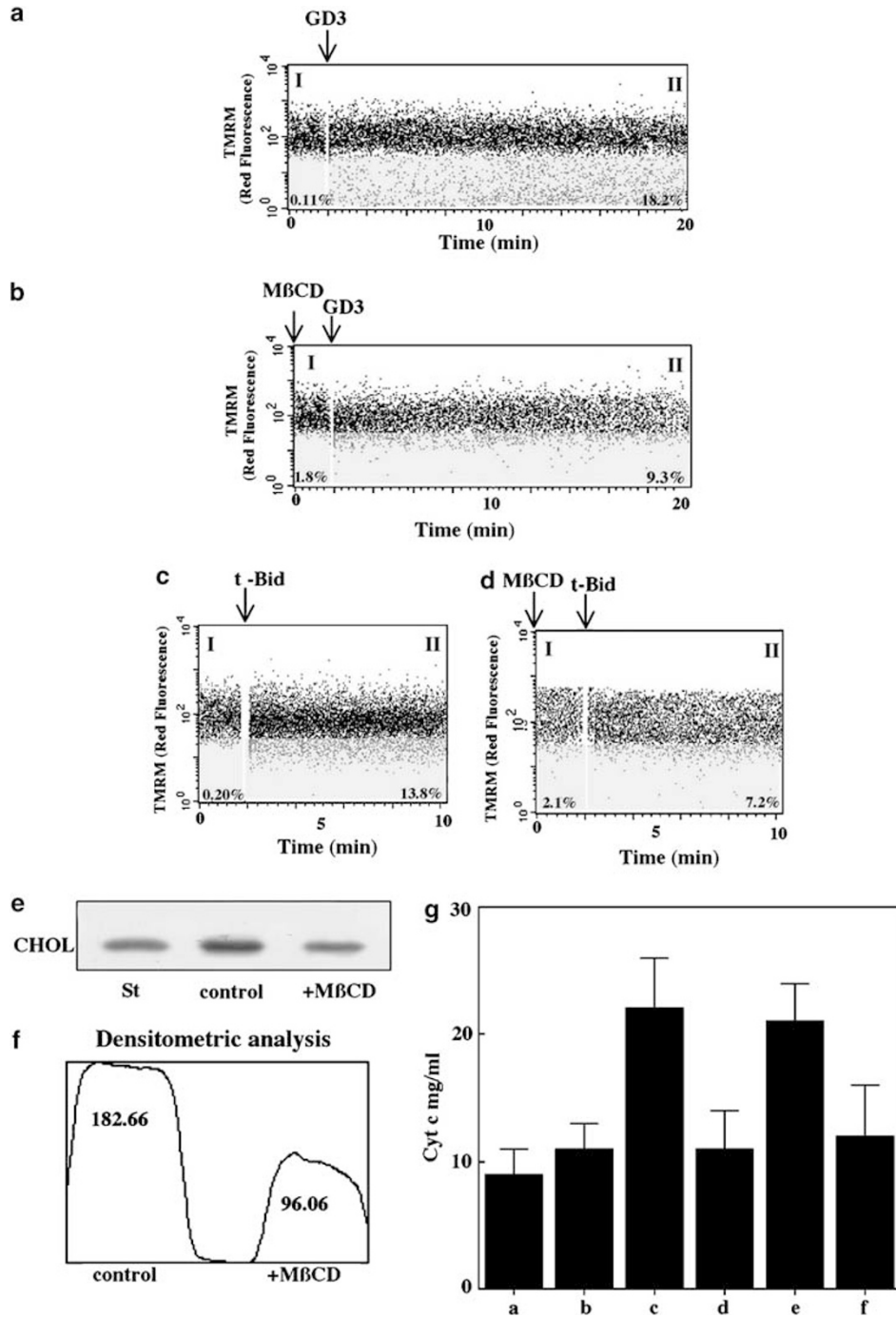


**Figure 6** Effect of  $M\beta CD$  on mitochondria depolarization induced by GD3 or t-Bid. Rapid changes occurring in membrane potential ( $\Delta\Psi$ ) of isolated mitochondria were quantified by cytofluorimetric analyses using TMRM ( $10\ \mu M$ ). (a) At 2 min after starting  $\Delta\Psi$  evaluations, considered as control sample (region I), GD3 ( $40\ \mu M$ ) was added to isolated mitochondria (arrow) and changes in  $\Delta\Psi$  were analyzed for 20 min (region II). As shown in the dot plot region II, GD3 induced a significant  $\Delta\Psi$  loss with respect to control samples. (b) Preincubation (5 min) with microdomain disrupting agent  $M\beta CD$  (arrow, dot plot region I), which did not induce *per se* any change of  $\Delta\Psi$  (region I), prevented the loss of  $\Delta\Psi$  induced by GD3 (dot plot region II). (c) Analysis of isolated mitochondria incubated with t-Bid at  $30^\circ C$  for 1 h in the absence of  $M\beta CD$  indicated a significant percentage of depolarized mitochondria (dot plot region II). (d) Preincubation (5 min) with  $M\beta CD$  reduced the percentage of depolarized mitochondria (dot plot region II). Changes in  $\Delta\Psi$  were analyzed for 10 min. Numbers represent percentages of mitochondria with membrane depolarization. One experiment representative of six. (e) Isolated mitochondria were preincubated for 5 min at room temperature with  $M\beta CD$  ( $500\ \mu g/ml$ ). Free cholesterol (CHOL) was analyzed by TLC. (f) The bands corresponding to standard cholesterol (St) were quantified by densitometric scanning analysis. A significant decrease of cholesterol content was detectable in the presence of  $M\beta CD$  with respect to control samples. (g) Evaluation of Cyt c release by isolated mitochondria in control untreated samples (a), and after treatment with  $M\beta CD$  (b), GD3 (c), and t-Bid (e).  $M\beta CD$  administration was ineffective *per se* (b) but it was able to significantly impair Cyt c release induced by both GD3 (d) and t-Bid (f). One experiment representative of three is shown



mitochondrial lipid microdomains. In particular, Bax and t-Bid very efficiently alter the permeability transition pore complex function. However, the molecular mechanism of this increased permeability is still unknown. In addition to Bax-VDAC interaction, a recent model<sup>35</sup> suggests a profound remodeling of the mitochondrial inner membrane to mobilize 85% of the Cyt *c* that is trapped in the cristae and, then, a t-Bid- and Bax-mediated translocation of Cyt *c* across the mitochondrial outer membrane. Since t-Bid directly alters membrane curvature<sup>36</sup> and regulates targets that are involved in cristae remodeling, it is likely that t-Bid may regulate the activity of fission and fusion effector molecules.<sup>17</sup> On the other hand, mitochondria undergo rapid and excessive fission in the apoptotic process.<sup>37</sup> In particular, overexpression of the human fission protein hFis1, an integral protein of the outer mitochondrial membrane, triggers fission of mitochondria, Cyt *c* release and subsequent apoptosis.<sup>18,38</sup> Furthermore, Bax colocalizes at mitochondrial fission sites early in the apoptotic process,<sup>39</sup> linking proapoptotic members of the Bcl-2 family to the mitochondrial fission and fusion machinery. Thus, we analyzed the presence and the possible interaction of hFis1 with mitochondrial lipid microdomains. Our results clearly suggested that the profound remodeling of the mitochondrial inner membrane induced the lateral reorganization of mitochondrial lipid microdomains, bringing hFis1 together with GD3 containing microdomains.

In conclusion, our findings suggest a role for GD3 (and possibly GM3) as a structural component of the multimolecular complex, including VDAC-1, Bcl-2 family and fission proteins, involved in the opening of the mitochondrial permeability transition pore. It is conceivable that proteins such as Bax and t-Bid catalyze the restructuring of lipids to induce pore formation. The role of the ganglioside in this multimolecular system could be to facilitate the transient and local formation of inverted hexagonal structures in mitochondrial membrane that undergo the fission process. Mitochondrial lipid microdomains may thus represent preferential sites where specific key reactions can take place and be catalyzed, hijacking T cells toward their survival or death. This hypothesis is strongly supported by the observation that the disruption of lipid microdomains in isolated mitochondria by M $\beta$ CD prevented mitochondria depolarization induced by GD3 or t-Bid.

Altogether, these findings may also have a clinical relevance in terms of drug-delivery. In fact, cyclodextrins that exert their effects via the formation of noncovalent inclusion complexes are being used in an ever-increasing way to camouflage undesirable pharmaceutical characteristics or to improve therapeutic indices and site-targeted delivery of different drugs, including some nonsteroidal anti-inflammatory drugs. For instance, one of these drugs, nimesulide, induces apoptosis by a mechanism involving subcellular redistribution and interaction of Bax with Bid and VDAC.<sup>40</sup> Hence, our results, pointing to the key role of this complex within mitochondrial lipid microdomains in cell fate regulation mechanisms, could provide further insight in this field, and suggest that in drug preparations used in clinical practice, the combined effect on cell apoptosis of nonsteroidal anti-inflammatory drugs and  $\beta$ -cyclodextrins has to be carefully evaluated and tested.

## Materials and Methods

### Cells and apoptosis induction

Human lymphoblastoid CEM cells<sup>41</sup> were maintained in RPMI 1640 medium (Gibco-BRL, Life Technologies Italia, Milano, Italy), containing 10% fetal calf serum (FCS) plus 100 U/ml penicillin, 100 mg/ml streptomycin, at 37°C in a humidified 5% CO<sub>2</sub> atmosphere. Apoptosis was induced by incubating cells at a concentration of  $5 \times 10^5$  per ml in serum-free medium supplemented with insulin (5  $\mu$ g/l) and transferrin (5  $\mu$ g/l), and by adding anti-Fas (CD95) IgM MoAb (clone CH11, Upstate Biotechnology, Lake Placid, NY USA) at 250 ng/ml for different incubation times (1, 10, 20, 40 min, 1 h, 2 h, 4 h). After treatment, cells were collected and prepared for other procedures as described below.

### Preparation of isolated mitochondria

CEM cells were suspended in a calcium- and magnesium-free phosphate-buffered saline solution (PBS) and collected by centrifugation. The following steps were carried out according to Zamzami *et al.*<sup>42</sup>

After washing three times with PBS, cells were resuspended in Hemo-buffer (10 mM HEPES, pH 7.4; 1 mM ethylene glycol-bis-(aminoethyl ether) *N,N,N',N'*-tetraacetic acid (EGTA), 0.1 M sucrose, 5% bovine serum albumin (BSA), 1 mM phenylmethylsulfonyl fluoride (PMSF) and complete protease inhibitor cocktail (Roche, Indianapolis, IN, USA), and maintained for 10 min on ice. After this time, cells were homogenized with about 100 strokes of a teflon homogenizer with B-type pestle. The homogenates were centrifuged at  $1000 \times g$  for 10 min at 4°C to remove intact cells and nuclei, and the supernatants were further centrifuged at  $10\,000 \times g$  at 4°C for 10 min to precipitate the heavy membrane fractions (enriched in mitochondria). These fractions were then purified by standard differential centrifugation. The mitochondrial pellet obtained was resuspended in swelling buffer (SB) containing 0.1 M sucrose, 0.5 M sodium succinate, 50 mM EGTA at pH 7.4, 1 M phosphoric acid (H<sub>3</sub>PO<sub>4</sub>), 0.5 M 3[*N*-Morpholino] butane-sulfonic acid (MOPS) and 2 mM Rotenone, kept on ice and used within 2 h from the preparation.

The purity of mitochondria preparation was assessed by Western blot by checking LAMP-1, GM-130, transferrin receptor (CD71) and subunit IV of cytochrome *c* oxidase (COX-4), using specific MoAbs (anti-LAMP-1, BD Pharmingen, San Diego, CA, USA; anti-GM-130, Molecular Probes, Eugene, OR, USA; anti-CD71, BD Pharmingen, and anti-COX-4, Molecular Probes). Protein content was determined by the Bicinchoninic Acid Method (Bio-Rad, Richmond, CA, USA). Mitochondria were kept on ice and used within 2 h of preparation.

### Analysis of mitochondrial GD3 localization by scanning confocal microscopy

CEM cells were fixed with 4% formaldehyde in PBS for 30 min at 4°C and labeled with GMR19 anti-GD3 MoAb (Seikagaku Corp., Chuo-ku, Tokyo, Japan)<sup>43</sup> for 1 h at 4°C, followed by three washes in PBS and addition (1 h at 4°C) of Texas Red-conjugated anti-mouse IgM (Calbiochem, La Jolla, CA, USA). In parallel experiments, CEM cells were directly stained with Mito Tracker Green FM (Molecular Probes) for 2 h at 37°C and then stimulated with anti-Fas for 1 h at 37°C, as reported above. Both untreated and Fas-stimulated cells were fixed with 4% paraformaldehyde in PBS for 30 min at room temperature and then permeabilized with 0.5% Triton X-100 in PBS for 5 min at room temperature, as previously reported.<sup>6</sup> Alternatively, cells were fixed with acetone-methanol (1 : 1, v/v) for 10 min at 4°C and then soaked in balanced salt solution (BSS; Sigma Chem. Co.).

Cells were stained with GMR19 anti-GD3 MoAb for 1 h at 4°C, followed by three washes in PBS and addition (1 h at 4°C) of Texas Red-conjugated anti-mouse IgM (Calbiochem). In parallel experiments, cells were stained with anti-GD3 MoAb before fixation. After incubation, the cells were washed three times with PBS and then resuspended in 0.1 M Tris-HCl, pH 9.2, containing 60% glycerol (v : v). The images were acquired with a Leica TCS SP2 confocal laser scanning microscope, usually with a  $\times 40$  objective. Acquisition of single fluorescein isothiocyanate (FITC) stained samples in dual fluorescence scanning configuration did not show contribution of green signal in red. Images were collected at  $512 \times 512$  pixels and processed with the Leica confocal software 4.7.

### Ganglioside extraction and analysis by high-performance thin layer chromatography (HPTLC)

Isolated mitochondria as well as supernatant withdrawn from mitochondria from CEM cells, either untreated or treated with anti-CD95/Fas, were subjected to ganglioside extraction according to the method of Svennerholm and Fredman,<sup>44</sup> with minor modifications. Samples were normalized for protein content, determined as described above. Briefly, samples were extracted twice in chloroform:methanol:water (4:8:3) (v : v : v) and subjected to Folch partition by the addition of water resulting in a final chloroform : methanol : water ratio of 1 : 2 : 1.4. The upper phase, containing polar glycosphingolipids, was purified of salts and low molecular weight contaminants using Bond elut C18 columns (Superchrom, Milan, Italy), according to the method of Williams and McCluer.<sup>45</sup> The eluted glycosphingolipids were dried down and separated by HPTLC, using silica gel 60 HPTLC plates (Merck, Darmstadt, Germany). Chromatography was performed in chloroform:methanol:0.25% aqueous KCl (5:4:1) (v : v : v). Plates were then air-dried and gangliosides visualized with resorcinol.<sup>46</sup> Alternatively, the ganglioside extract was run on HPTLC aluminium-backed silica gel 60 (20  $\times$  20) plates (Merck). The plates were immunostained for 1 h at room temperature with GMR19 anti-GD3 MoAb (Seikagaku Corp.) and then with horseradish peroxidase (HRP)-conjugated anti-mouse IgM (Sigma Chem. Co.). Immunoreactivity was assessed by chemiluminescence reaction using the ECL Western detection system (Amersham Biosciences).

### Detection of GD3 microdomains by TEM

For TEM examination, CEM cells, untreated or treated with anti-CD95/Fas (250ng/ml for 1 h at 37°C), were fixed in 2.5% cacodylate-buffered (0.2 M, pH 7.2) glutaraldehyde for 20 min at room temperature and postfixed in 1% OsO<sub>4</sub> in cacodylate buffer for 1 h at room temperature. Fixed specimens were dehydrated through a graded series of ethanol solutions and embedded in Agar 100 (Agar Aids, Cambridge, UK). Serial ultrathin sections were collected on 200-mesh grids. Thin sections were then treated with PBS containing 1% (w/v) gelatin, 1% BSA, 5% FCS and 0.05% Tween-20 and then incubated with GMR19 anti-GD3 MoAb (Seikagaku Corp.) diluted 1:30 in the same buffer without gelatin overnight at 4°C. After washing for 1 h at room temperature, sections were labeled with anti-mouse IgM-10 nm gold conjugate (1 : 10) for 1 h at room temperature and washed again. Negative controls were incubated with the gold conjugate alone and then counterstained with uranyl acetate and lead citrate. Sections were observed with a Philips 208 electron microscope at 80 kV. TEM morphometric analyses were carried out by evaluating at least 100 different cells detected on different thin sections at the same magnification ( $\times 16000$ ) coming from three separated experiments. Plasma membrane, cytoplasmic and mitochondrial gold particles were

assessed in control and anti-CD95/Fas treated cells. Statistical evaluations were performed by using Student's *t*-test analyses (statview software for Macintosh computer).

### Ganglioside analysis in the immunoprecipitates of the VDAC-1

Briefly, CEM cells, untreated or treated with anti-CD95/Fas (250 ng/ml for 1 h at 37°C), were lysed in lysis buffer (10 mM Tris-HCl (pH 8.0), 150 mM NaCl, 1% Nonidet P-40, 1 mM PMSF, 10 mg of leupeptin/ml). Cell-free lysates were mixed with protein A-acrylic beads and stirred by a rotary shaker for 2 h at 4°C to preclude nonspecific binding. After centrifugation (500  $\times g$  for 1 min), the supernatant was immunoprecipitated with goat anti-VDAC/porin (N18 Santa Cruz Biotechnologies) or, alternatively, with anti-Bid polyclonal Ab (RD Systems Inc., Minneapolis, MN, USA) plus protein A-acrylic beads. A goat or, alternatively, a rabbit IgG isotypic control (Sigma Chem. Co.) was employed.

The immunoprecipitates were subjected to ganglioside extraction, as reported above. The ganglioside extract was split into two aliquots. The first one was run on silica gel 60 HPTLC plates (Merck) and stained by resorcinol to detect the complete ganglioside pattern of the immunoprecipitates. The second one was run on HPTLC aluminium-backed silica gel 60 (20  $\times$  20) plates (Merck), as reported above. The plates were immunostained for 1 h at room temperature with GMR19 anti-GD3 MoAb (Seikagaku Corp.) and then with HRP-conjugated anti-mouse IgM (Sigma Chem. Co.). Immunoreactivity was assessed by chemiluminescence reaction using the ECL Western detection system (Amersham Biosciences). Protein loading was evaluated by India ink staining.<sup>47</sup>

### Isolation and analysis of GEM fraction

GEM fraction from lymphoblastoid CEM cells, either untreated or treated with anti-CD95/Fas, was isolated as previously described.<sup>48</sup> The optimal incubation time with anti-CD95/Fas (1 h at 37°C) was selected on the basis of preliminary experiments. Briefly,  $2 \times 10^8$  cells were suspended in 1 ml of lysis buffer, containing 1% Triton-X-100, 10 mM Tris-HCl (pH 7.5), 150 mM NaCl, 5 mM EDTA, 1 mM NaVO<sub>4</sub> and 75 U of aprotinin and allowed to stand for 20 min. The cell suspension was mechanically disrupted by Dounce homogenization (10 strokes). The lysate was centrifuged for 5 min at 1300  $\times g$  to remove nuclei and large cellular debris. The supernatant fraction (postnuclear fraction) was subjected to sucrose density gradient centrifugation, that is, the fraction was mixed with an equal volume of 85% sucrose (w/v) in lysis buffer (10 mM Tris-HCl, pH 7.5, 150 mM NaCl, 5 mM EDTA). The resulting diluent was placed at the bottom of a linear sucrose gradient (5–30%) in the same buffer and centrifuged at 200 000  $\times g$  for 16–18 h at 4°C in a SW41 rotor (Beckman Inst., Palo Alto, CA, USA). After centrifugation, the gradient was fractionated, and 11 fractions were collected starting from the top of the tube. All steps were carried out at 0–4°C.

Alternatively, mitochondria isolated from the same cells as above either untreated or treated with anti-CD95/Fas were detergent solubilized according to Skibbens *et al.*<sup>49</sup> Briefly, mitochondria were lysed with 1 ml of extraction buffer (25 mM HEPES, pH 7.5, 0.15 NaCl, 1% Triton X-100 and 100 kallikrein U/ml aprotinin) for 20 min on ice. Lysates were collected and centrifuged for 2 min in a Brinkmann microfuge at 12 000 rpm at 4°C. Supernatants, containing Triton X-100 soluble material, were collected; pellets were undertaken to a second centrifugation (30 s) in order to remove the remaining soluble material. The pellets were then solubilized in 100  $\mu$ l of buffer containing 50 mM Tris-HCl, pH 8.8, 5 mM EDTA and 1%

SDS. DNA was sheared by passage through a 22 ga. needle. Both Triton X-100 soluble and -insoluble material were analyzed by Western blot as described above.

The amount of protein in each fraction was first quantified as described above. Finally, all the fractions from untreated and CD95/Fas-stimulated cells were subjected to Western blot analysis.

### Immunoblotting analysis of GEM fraction

All the fractions obtained as reported above were subjected to 15% sodium-dodecyl sulphate polyacrylamide gel electrophoresis (SDS-PAGE). The proteins were electrophoretically transferred onto polyvinylidene difluoride (PVDF) membranes (Bio-Rad). Membranes were blocked with 5% defatted dried milk in TBS containing 0.05% Tween-20 and probed with anti-VDAC-1/porin polyclonal Ab (N18, Santa Cruz Biotechnologies, Santa Cruz, CA, USA), anti-Bid polyclonal Ab (RD Systems Inc.), anti-hFis1 polyclonal Ab (Alexis Biochemicals, San Diego, CA, USA), or anti-Bax MoAb (Santa Cruz Biotechnologies). Bound antibodies were visualized with HRP-conjugated anti-goat IgG, anti-rabbit IgG or anti-mouse IgG (Sigma Chem. Co.) and immunoreactivity assessed by chemiluminescence reaction using the ECL Western blocking detection system (Amersham, Buckinghamshire, UK).

Densitometric scanning analysis was performed by Mac OS 9.0 (Apple Computer International), using NIH Image 1.62 software.

### Immunofluorescence and intensified video microscopy

CEM cells were prestained with Mito Tracker Green FM (200 nM) (Molecular Probes) for 2 h at 37°C and then stimulated with anti-CD95/Fas (250 ng/ml for 1 h at 37°C), as reported above. Control and treated cells were collected by centrifugation, allowed to attach to glass coverslips precoated with polylysine and fixed with 4% paraformaldehyde in PBS for 30 min at room temperature. After washing in the same buffer, cells were permeabilized with 0.5% Triton X-100. Samples were incubated at 37°C for 30 min with polyclonal antibodies to hFis1 (Alexis Biochemicals) and then with Texas Red-conjugated anti-rabbit IgG (Alexa Fluor 594, Molecular Probes). Alternatively, cells were incubated with polyclonal antibodies to hFis1 plus Texas Red-conjugated anti-rabbit IgG and then with GMR19 anti-GD3 MoAb (Seikagaku Corporation) plus Texas Red-conjugated anti-mouse IgM (Alexa Fluor 594, Molecular Probes). After washing, all samples were mounted with glycerol:PBS (2:1) and observed with a Nikon Microphot fluorescence microscope. Images were captured by a color chilled 3CCD camera (Hamamatsu, Japan). Normalization and background subtraction were performed for each image. Figures were obtained by the OPTILAB (Graftek, France) software for image analysis.

### Analysis of the effect of M $\beta$ CD on mitochondria depolarization induced by GD3 or t-Bid

Isolated mitochondria were resuspended in SB (0.5 mg/ml) at the final volume of 1.5 ml.<sup>2</sup> The  $\Delta\Psi$  of isolated mitochondria was quantified by cytofluorimetric analysis after mitochondria staining with 1  $\mu$ M tetramethylrhodamine-methyl-ester-perchlorate (TMRM; Molecular Probes), a potential sensitive probe: low levels of TMRM incorporation (revealed by a decrease of red fluorescence) indicated a low  $\Delta\Psi$ . As a positive control, 300  $\mu$ M Ca<sup>2+</sup> was employed. To verify the quality of mitochondrial

preparations for each experiment, controls were performed to assess the background incorporation of fluorochromes for 3 min.

In the first set of experiments, 40  $\mu$ M GD3 (Alexis Biochemicals) or 1  $\mu$ g/ml t-Bid (kindly provided by Dr. Mauro Degli Esposti, University of Manchester, UK)<sup>50</sup> was added to the mitochondrial preparation and immediately analyzed by flow cytometer for 20 min. In parallel experiments, samples were preincubated for 5 min at room temperature with microdomain disrupting agent M $\beta$ CD (500  $\mu$ g/ml) (Sigma Chem Co.) in the presence or in the absence of either GD3 or t-Bid. Total recording times was 20 min. The amount of cholesterol was evaluated as described previously.<sup>51</sup> Free cholesterol was quantified from TLC plates by densitometric scanning and comparison with standard. The density of the bands used to quantitate cholesterol concentration fell within the linear range of compound concentration *versus* absorbance. Cyt *c* was evaluated in supernatants from isolated mitochondria by a sensitive and specific immunoassay, using a commercial ELISA kit (R&D System), according to the manufacturer's instructions. The light emitted was quantified by using a microtiter plate reader at 405 nm. CytC concentration was expressed as ng/ml.

The  $\Delta\Psi$  of isolated mitochondria was quantified by cytofluorimetric analysis, using a FACScan cytometer (Becton Dickinson, Mountain View, CA, USA) equipped with a 488 argon laser. To exclude debris, during analyses samples were gated based on light scattering properties in the side scattering (SSC) and forward scattering (FSC) modes. Dot plots were statistically analyzed by using CellQuest software for Macintosh computer (BD) in order to determine the percentage of mitochondria with depolarized membrane.

### Acknowledgements

We thank Dr. Mauro Degli Esposti, University of Manchester, UK; Dr. Stefano Rufini, University of Rome 'Tor Vergata', Italy; and Dr. Paola Matarrese, Istituto Superiore di Sanità, Rome, Italy, for helpful suggestions and criticisms. This work was supported by grants from Ministero della Salute, Italy to MS AP and WM.

### References

1. Ardail D, Popa I, Bodennee J, Louisot P, Schmitt D and Portoukalian J (2003) The mitochondria-associated endoplasmic-reticulum subcompartment (MAM fraction) of rat liver contains highly active sphingolipid-specific glycosyltransferases. *Biochem. J.* 371: 1013–1019
2. Birbes H, El Bawab S, Hannun YA and Obeid LM (2001) A mitochondrial pool of sphingomyelin is involved in TNF $\alpha$ -induced Bax translocation to mitochondria. *FASEB J.* 14: 2669–2679
3. Kiguchi K, Henning-Chubb BC and Huberman E (1990) Glycosphingolipid patterns of peripheral blood lymphocytes, monocytes, and granulocytes are cell specific. *J. Biochem. (Tokyo)* 107: 8–14
4. Pizzo P and Viola A (2003) Lymphocyte lipid rafts: structure and function. *Curr. Opin. Immunol.* 15: 255–260
5. Garofalo T, Lenti L, Longo A, Misasi R, Mattei V, Pontieri GM, Pavan A and Sorice M (2002) Association of GM3 with Zap-70 induced by T cell activation in plasma membrane microdomains: GM3 as a marker of microdomains in human lymphocytes. *J. Biol. Chem.* 277: 11233–11238
6. Garofalo T, Misasi R, Mattei V, Giammarioli AM, Malorni W, Pontieri GM, Pavan A and Sorice M (2003) Association of the death-inducing signaling complex with microdomains after triggering through CD95/Fas. Evidence for caspase-8-ganglioside interaction in T cells. *J. Biol. Chem.* 278: 8309–8315
7. Muppidi JR and Siegel RM (2004) Ligand-independent redistribution of Fas (CD95) into lipid rafts mediates clonotypic T cell death. *Nat. Immunol.* 5: 182–189

8. Algeciras-Schimmich A, Shen L, Barnhart BC, Murmann AE, Burkhardt JK and Peter ME (2002) Molecular ordering of the initial signaling events of CD95. *Mol. Cell. Biol.* 22: 207–220
9. Hueber AO, Bernard AM, Herincs Z, Couzinet A and He HT (2002) An essential role for membrane rafts in the initiation of Fas/CD95-triggered cell death in mouse thymocytes. *EMBO Rep.* 3: 190–196
10. De Maria R, Lenti L, Malisan F, d'Agostino F, Tomassini B, Zeuner A, Rippo MR and Testi R (1997) Requirement for GD3 ganglioside in CD95- and ceramide-induced apoptosis. *Science* 277: 1652–1655
11. Giammarioli AM, Garofalo T, Sorice M, Misasi R, Gambardella L, Gradini R, Fais S, Pavan A and Malorni W (2001) GD3 glycosphingolipid contributes to Fas-mediated apoptosis via association with ezrin cytoskeletal protein. *FEBS Lett.* 506: 45–50
12. Ikonen E (2001) Roles of lipid rafts in membrane transport. *Curr. Opin. Cell Biol.* 13: 470–477
13. Garcia-Ruiz C, Colell A, Morales A, Calva M, Enrich C and Fernandez-Checa JC (2002) Trafficking of ganglioside GD3 to mitochondria by tumor necrosis factor- $\alpha$ . *J. Biol. Chem.* 277: 36443–36448
14. De Maria R, Rippo MR, Schuchman HE and Testi R (1998) Acidic sphingomyelinase (ASM) is necessary for fas-induced GD3 ganglioside accumulation and efficient apoptosis of lymphoid cells. *J. Exp. Med.* 187: 897–902
15. Rippo MR, Malisan F, Ravagnan L, Tomassini B, Condo I, Costantini P, Susin SA, Rufini A, Todaro M, Kroemer G and Testi R (2000) GD3 ganglioside directly targets mitochondria in a bcl-2-controlled fashion. *FASEB J.* 14: 2047–2054
16. Garcia-Ruiz C, Colell A, Paris R and Fernandez-Checa JC (2000) Direct interaction of GD3 ganglioside with mitochondria generates reactive oxygen species followed by mitochondrial permeability transition, cytochrome *c* release, and caspase activation. *FASEB J.* 14: 847–858
17. Karbowski M and Youle RJ (2003) Caspase inhibition prevents the mitochondrial release of apoptosis-inducing factor. *Cell Death Differ.* 10: 870–880
18. Matarrese P, Tinari A, Mormone E, Bianco GA, Toscano MA, Ascione B, Rabinovich GA and Malorni W (2005) Galectin-1 sensitizes resting human T lymphocytes to Fas (CD95)-mediated cell death via mitochondrial hyperpolarization, budding, and fission. *J. Biol. Chem.* 280: 6969–6985
19. van Blitterswijk WJ, van der Luit AH, Veldman RJ, Verheij M and Borst J (2003) Ceramide: second messenger or modulator of membrane structure and dynamics? *Biochem. J.* 369: 199–211
20. Misasi R, Sorice M, Garofalo T, Griggi T, Giammarioli AM, d'Ettore G, Vullo V, Pontieri GM, Malorni W and Pavan A (2000) Overexpression of lymphocytic GD3 ganglioside and presence of anti-GD3 antibodies in patients with HIV infection. *AIDS Res. Hum. Retroviruses* 16: 1539–1549
21. Scorrano L, Petronilli V, Di Lisa F and Bernardi P (1999) Commitment to apoptosis by GD3 ganglioside depends on opening of the mitochondrial permeability transition pore. *J. Biol. Chem.* 274: 22581–22585
22. Cheng EHY, Sheiko TV, Fisher JK, Craigen WJ and Korsmeyer SJ (2003) VDAC2 inhibits BAK activation and mitochondrial apoptosis. *Science* 301: 513–517
23. Sorice M, Circella A, Cristea IM, Garofalo T, Di Renzo L, Alessandri C, Valesini G and Degli Esposti MD (2004) Cardiolipin and its metabolites move from mitochondria to other cellular membranes during death receptor-mediated apoptosis. *Cell Death Differ.* 11: 1133–1145
24. Wei MC, Zong WX, Cheng EH, Lindsten T, Panoutsakopoulou V, Ross AJ, Roth KA, MacGregor GR, Thompson CB and Korsmeyer SJ (2001) Proapoptotic BAX and BAK: a requisite gateway to mitochondrial dysfunction and death. *Science* 292: 727–730
25. Shimizu S, Narita M and Tsujimoto Y (1999) Bcl-2 family proteins regulate the release of apoptogenic cytochrome *c* by the mitochondrial channel VDAC. *Nature* 399: 483–487
26. Shimizu S, Ide T, Yanagida T and Tsujimoto Y (2000) Electrophysiological study of a novel large pore formed by Bax and the voltage-dependent anion channel that is permeable to cytochrome *c*. *J. Biol. Chem.* 275: 12321–12325
27. Kim TH, Zhao Y, Ding WX, Shin JN, He X, Seo YW, Chen J, Rabinowich H, Amoscato AA and Yin XM (2004) Bid-cardiolipin interaction at mitochondrial contact site contributes to mitochondrial cristae reorganization and cytochrome *C* release. *Mol. Biol. Cell* 15: 3061–3072
28. Lange Y (1991) Disposition of intracellular cholesterol in human fibroblasts. *J. Lipid Res.* 32: 329–339
29. Van Meer G (1989) Lipid traffic in animal cells. *Annu. Rev. Cell Biol.* 5: 247–275
30. Simons K and Ikonen E (1997) Functional rafts in cell membranes. *Nature* 387: 569–572
31. Ayllon V, Fleischer A, Cayla X, Garcia A and Rebollo A (2002) Segregation of Bad from lipid rafts is implicated in the induction of apoptosis. *J. Immunol.* 168: 3387–3393
32. Fleischer A, Ghadiri A, Dessauge F, Duhamel M, Cayla X, Garcia A and Rebollo A (2004) Bad-dependent rafts alteration is a consequence of an early intracellular signal triggered by interleukin-4 deprivation. *Mol. Cancer Res.* 2: 674–684
33. Gajate C, Del Canto-Janez E and Acuna AU (2004) Intracellular triggering of Fas aggregation and recruitment of apoptotic molecules into Fas-enriched rafts in selective tumor apoptosis. *J. Exp. Med.* 200: 356–365
34. Nicholson DW and McMurray WC (1986) Triton solubilization of proteins from pig liver mitochondrial membranes. *Biochim. Biophys. Acta* 856: 515–525
35. Scorrano L, Ashiya M, Buttke K, Weiler S, Oakes SA, Mannella CA and Korsmeyer SJ (2002) A distinct pathway remodels mitochondrial cristae and mobilizes cytochrome *c* during apoptosis. *Dev. Cell* 2: 55–67
36. Epand RF, Martinou JC, Fornallaz-Mulhauser M, Hughes DW and Epand RM (2002) The apoptotic protein tBid promotes leakage by altering membrane curvature. *J. Biol. Chem.* 277: 32632–32639
37. Bossy-Wetzel E, Barsoum MJ, Godzik A, Schwarzenbacher R and Lipton SA (2003) Mitochondrial fission in apoptosis, neurodegeneration and aging. *Curr. Opin. Cell Biol.* 15: 706–716
38. James DI, Parone PA, Mattenberger Y and Martinou JC (2003) hFis1, a novel component of the mammalian mitochondrial fission machinery. *J. Biol. Chem.* 278: 36373–36379
39. Karbowski M, Lee YJ, Gaune B, Jeong SY, Frank S, Nechushtan A, Santel A, Fuller M, Smith CL and Youle RJ (2002) Spatial and temporal association of Bax with mitochondrial fission sites, Drp1, and Mfn2 during apoptosis. *J. Cell Biol.* 159: 931–938
40. Godlewski MM, Gajkowska B, Lamparska-Przybylska M and Motyl T (2002) Colocalization of BAX with BID and VDAC-1 in nimesulide-induced apoptosis of human colon adenocarcinoma COLO 205 cells. *Anti-Cancer Drugs* 13: 1017–1029
41. Foley GE, Lazarus H, Farber S, Uzman BG, Boone BA and McCarthy RE (1965) Continuous culture of human lymphoblasts from peripheral blood of a child with acute leukemia. *Cancer* 18: 522–529
42. Zamzami N, Maise C, Metivier D and Kroemer G (2001) Measurement of membrane permeability and permeability transition of mitochondria. *Methods Cell Biol.* 65: 147–158
43. Kotani M, Kawashima I, Ozawa H, Ogura K, Ishizuka I, Terashima T and Tai T (1994) Immunohistochemical localization of minor gangliosides in the rat central nervous system. *Glycobiology* 4: 855–865
44. Svennerholm L and Fredman PA (1980) A procedure for the quantitative isolation of brain gangliosides. *Biochim. Biophys. Acta* 617: 97–109
45. Williams MA and McCluer RH (1980) The use of Sep-Pak C18 cartridges during the isolation of gangliosides. *J. Neurochem.* 35: 266–269
46. Svennerholm L (1957) Quantitative estimation of sialic acids. II. A colorimetric resorcinol-hydrochloric acid method. *Biochim. Biophys. Acta* 24: 604–611
47. Hancock K and Tsang VC (1983) India ink staining of proteins on nitrocellulose paper. *Anal. Biochem.* 133: 157–162
48. Rodgers W and Rose JK (1996) Exclusion of CD45 inhibits activity of p56lck associated with glycolipid-enriched membrane domains. *J. Cell Biol.* 135: 1515–1523
49. Skibbens JE, Roth MG and Matlin KS (1989) Differential extractability of influenza virus hemagglutinin during intracellular transport in polarized epithelial cells and nonpolar fibroblasts. *J. Cell Biol.* 108: 821–832
50. Degli Esposti M, Ferry G, Masdehors P, Boutin JA, Hickman JA and Dive C (2003) Post-translational modification of Bid has differential effects on its susceptibility to cleavage by caspase 8 or caspase 3. *J. Biol. Chem.* 278: 15749–15757
51. Huber LA, Xu Q, Jurgens G, Bock G, Buhler E, Gey KF, Schonitzer D, Trall KN and Wick G (1991) Correlation of lymphocyte lipid composition membrane microviscosity and mitogen response in the aged. *Eur. J. Immunol.* 21: 2761–2765